

## Hollow Single-Crystal Spinel Nanocubes: The Case of Zinc Cobalt Oxide Grown by a Unique Kirkendall Effect

Li Tian,<sup>†</sup> Xianfeng Yang,<sup>†</sup> Ping Lu,<sup>‡</sup> Ian D. Williams,<sup>§</sup> Caihong Wang,<sup>†</sup> Shunying Ou,<sup>†</sup> Chaolun Liang,<sup>†</sup> and Mingmei Wu<sup>\*†</sup>

State Key Laboratory of Optoelectronic Materials and Technology/MOE Key Laboratory of Bioinorganic and Synthetic Chemistry, School of Chemistry and Chemical Engineering, and Instrumental Analysis and Research Center, Sun Yat-Sen (Zhongshan) University, Guangzhou 510275, People's Republic of China, Department of Materials Science and Engineering, New Mexico Institute of Mining and Technology, Socorro, New Mexico 87801, and Department of Chemistry, Hong Kong University of Science and Technology, Clear Water Bay, Kowloon, Hong Kong, People's Republic of China

Received December 19, 2007

Small hollow nanocubes of the ternary spinel  $Zn_xCo_{1-x}Co_2O_4$  of ca. 18 nm dimension were prepared via a facile hydrothermal route. A growth mechanism is suggested in which solid single-crystal  $Co_3O_4$  nanocubes are gradually converted to hollow single-crystal  $Zn_xCo_{1-x}Co_2O_4$  nanocubes with preservation of the spinel framework through differential diffusion of  $Zn^{2+}$  and  $Co^{2+}$  ions. With the cation exchange, the chemical composition and thus physical properties can be tailored.

In the past decade, increasing efforts have been made to prepare hollow nanostructures of electronic, optical, and magnetic materials due to a range of potential technological applications.<sup>1–17</sup> Various template-based strategies have been developed for the preparation of inorganic hollow nanomaterials.<sup>1</sup> While nonreactive hard templates were normally used to define the physical geometrical structure, reactive templates have been used for controlling both the shape and composition of derivative hollow nanostructures through

appropriate chemical transformations,<sup>1</sup> such as via the interior corrosion,<sup>8</sup> Ostwald ripening,<sup>6,12</sup> and Kirkendall diffusion.<sup>2,5,15–17</sup> The Kirkendall effect, a classical phenomenon in metallurgy,<sup>16</sup> was recently employed for the formation of a wide range of hollow spherical, polyhedral, and tubular nanostructures.<sup>1,5,15–17</sup> The method makes use of differential diffusion rates between two components in a diffusion couple to form an interior cavity. In this method, the precursor can serve as both a site template and a reactant.<sup>16</sup> However, during the formation of hollow structures, the chemical reactions on the precursor crystals inevitably lead to a change of the crystal geometry and thus often result in multifaceted or spherical shells, which are different from those of the starting crystals.<sup>4,5</sup> Although claims have been made that the

\* To whom correspondence should be addressed. E-mail: ceswmm@mail.sysu.edu.cn.

<sup>†</sup> Sun Yat-Sen (Zhongshan) University.

<sup>‡</sup> New Mexico Institute of Mining and Technology.

<sup>§</sup> Hong Kong University of Science and Technology.

- (1) Jeong, U.; Wang, Y. L.; Ibisate, M.; Xia, Y. N. *Adv. Funct. Mater.* **2005**, *15*, 1907–1921. (b) Zeng, H. C. *J. Mater. Chem.* **2006**, *16*, 649–662.
- (2) (a) Yin, Y. D.; Rioux, R. M.; Erdonmez, C. K.; Hughes, S.; Somorjai, G. A.; Alivisatos, A. P. *Science* **2004**, *304*, 711–714. (b) Chiang, R. K.; Chiang, R. T. *Inorg. Chem.* **2007**, *46*, 369–371. (c) Henkes, A. E.; Vasquez, Y.; Schaak, R. E. *J. Am. Chem. Soc.* **2007**, *129*, 1896–1897. (d) Chou, N. H.; Schaak, R. E. *J. Am. Chem. Soc.* **2007**, *129*, 7339–7345. (e) Gao, P. X.; Wang, Z. L. *J. Am. Chem. Soc.* **2003**, *125*, 11299–11305.
- (3) Fan, H. J.; Knez, M.; Scholz, R.; Nielsch, K.; Pippel, E.; Hesse, D.; Zacharias, M.; Gösele, U. *Nat. Mater.* **2006**, *5*, 627–631.
- (4) (a) Ding, S.; Lu, P.; Zheng, J. G.; Yang, X. F.; Zhao, F. L.; Chen, J.; Wu, H.; Wu, M. M. *Adv. Funct. Mater.* **2007**, *17*, 1879–1886. (b) Cao, H. L.; Qian, X. F.; Wang, C.; Ma, X. D.; Yin, J.; Zhu, Z. K. *J. Am. Chem. Soc.* **2005**, *127*, 16024–16025.
- (5) (a) Jiao, S. H.; Xu, L. F.; Jiang, K.; Xu, D. S. *Adv. Mater.* **2006**, *18*, 1174–1177. (b) Cao, H. L.; Qian, X. F.; Zai, J. T.; Yin, J.; Zhu, Z. K. *Chem. Commun.* **2006**, *43*, 4548–4550.

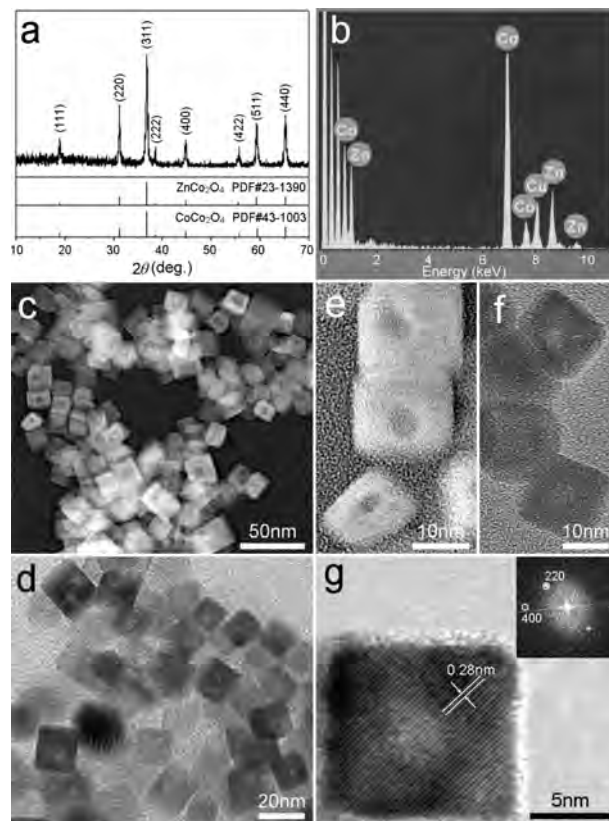
- (6) Teo, J. J.; Chang, Y.; Zeng, H. C. *Langmuir* **2006**, *22*, 7369–7377.
- (7) Yang, J. H.; Qi, L. M.; Lu, C. H.; Ma, J. M.; Cheng, H. M. *Angew. Chem., Int. Ed.* **2005**, *44*, 598–603.
- (8) (a) Xiong, Y. J.; Wiley, B.; Chen, J. Y.; Li, Z. Y.; Yin, Y. D.; Xia, Y. N. *Angew. Chem., Int. Ed.* **2005**, *44*, 7913–7917. (b) Kim, D.; Park, J.; An, K.; Yang, N. K.; Park, J. G.; Hyeon, T. *J. Am. Chem. Soc.* **2007**, *129*, 5812–5813.
- (9) (a) Sun, Y. G.; Xia, Y. N. *Science* **2002**, *298*, 2176–2179. (b) Lu, C. H.; Qi, L. M.; Yang, J. H.; Wang, X. Y.; Zhang, D. Y.; Xie, J. L.; Ma, J. M. *Adv. Mater.* **2005**, *17*, 2562–2567. (c) Jiang, Z. Y.; Xie, Z. X.; Zhang, X. H.; Lin, S. C.; Xu, T.; Xie, S. Y.; Huang, R. B.; Zheng, L. S. *Adv. Mater.* **2004**, *16*, 904–907. (d) Son, D. H.; Hughes, S. M.; Yin, Y. D.; Alivisatos, A. P. *Science* **2004**, *306*, 1009–1012. (e) Caruso, F.; Caruso, R. A.; Mohwald, H. *Science* **1998**, *282*, 1111–1114.
- (10) Wang, W. Z.; Poudel, B.; Wang, D. Z.; Ren, Z. F. *Adv. Mater.* **2005**, *17*, 2110–2114.
- (11) He, T.; Chen, D. R.; Jiao, X. L.; Wang, Y. L. *Adv. Mater.* **2006**, *18*, 1078–1082.
- (12) Yu, J. G.; Guo, H. T.; Davis, S. A.; Mann, S. *Adv. Funct. Mater.* **2006**, *16*, 2035–2041.
- (13) Li, X. H.; Zhang, D. H.; Chen, J. S. *J. Am. Chem. Soc.* **2006**, *128*, 8382–8383.
- (14) Li, H. X.; Bian, Z. F.; Zhu, J.; Zhang, D. Q.; Li, G. S.; Huo, Y. N.; Li, H.; Lu, Y. F. *J. Am. Chem. Soc.* **2007**, *129*, 8406–8407.
- (15) Dloczik, L.; Kolnenkamp, R. *Nano Lett.* **2003**, *3*, 651–653.
- (16) Fan, H. J.; Gösele, U.; Zacharias, M. *Small* **2007**, *3*, 1660–1671.
- (17) Li, Y. G.; Tan, B.; Wu, Y. Y. *J. Am. Chem. Soc.* **2006**, *128*, 14258–14259.

morphology could be preserved during hollowing, changes in the wall structure were evident in the previous works because of mass transport and/or phase change.<sup>5</sup>

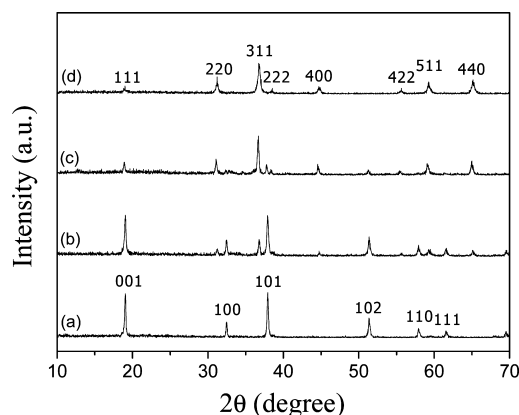
Among hollow nanostructures, examples of hollow single-crystal cubes are extremely rare for compounds. The only reported examples are related to binary PbTe<sup>10</sup> and Cu<sub>2</sub>O (CuO).<sup>5,6</sup> AB<sub>2</sub>O<sub>4</sub>-type spinel oxides of cubic symmetry are a large family of natural and synthetic compounds.<sup>13,17–20</sup> Kirkendall diffusion has been previously used to synthesize single-crystal spinel ZnAl<sub>2</sub>O<sub>4</sub> nanotubes from ZnO via an interfacial solid-state reaction with Al<sub>2</sub>O<sub>3</sub> at high temperature.<sup>3</sup> Growth of hollow submicron cubes built by spinel Co<sub>3</sub>O<sub>4</sub> nanocrystals has also been achieved by a surfactant-template route.<sup>11</sup> In this paper, we present hollow single-crystal spinel nanocubes and provide evidence for their formation in an aqueous solution by nanoscale Kirkendall diffusion. The product for this study is a ternary spinel compound: zinc cobalt oxide.

Figure 1a shows the result of powder X-ray diffraction (XRD) pattern for the product obtained after a facile autoclaving process at 180 °C for 24 h. The details of experiments are given in the Supporting Information. The pattern is in close agreement to the standard XRD patterns of spinels CoCo<sub>2</sub>O<sub>4</sub> (JCPDS no. 43-1003) and ZnCo<sub>2</sub>O<sub>4</sub> (JCPDS no. 23-1390). The zinc/cobalt ratio in the spinel nanopowder was then determined to be ca. 1:3 by energy-dispersive X-ray spectroscopy (EDS; Figure 1b). The composition corresponds to the spinel solid solution Zn<sub>x</sub>Co<sub>1-x</sub>Co<sub>2</sub>O<sub>4</sub> with *x* of ca. 0.75. The crystals with the cube geometry in the product have a mean edge length of ca. 18 nm (Figure 1c–g). The remarkable contrast between the cube edges and centers observed in both dark- and bright-field transmission electron microscopy (TEM) images indicates the hollow nature of the cubes. The cubes have a wall thickness of ca. 6 nm. To the best of our knowledge, these are the smallest hollow nanocubes of any compound reported to date. The lattice fringe of 0.28 nm spacing in the high-resolution TEM (HRTEM) image (Figure 1g) corresponds well to the *d* spacing of the {220} lattice planes. The fast Fourier transformation (FFT) pattern in Figure 1g indicates that the hollow nanocubes are single crystal and bound by primary {100} facets.

To understand the growth mechanism of the hollow nanocubes, a detailed time-dependent crystallization study was carried out. Figure 2 shows the powder XRD patterns of the products obtained after different reaction times. The



**Figure 1.** (a) XRD pattern of the product grown for 24 h. (b) EDS spectrum obtained under TEM observation. (c and d) Low-magnification dark- and bright-field TEM images, respectively. (e and f) High-magnification dark- and bright-field TEM images, respectively. (g) HRTEM image of a single hollow nanocube along with its FFT (inset).



**Figure 2.** Powder XRD patterns of the products prepared at 180 °C for (a) 3.0, (b) 6.0, (c) 12, and (d) 18 h.

sole solid product after 3.0 h of reaction is hexagonal  $\beta$ -Co(OH)<sub>2</sub>, which has a brucite-like structure (JCPDS no. 30-0443; *a* = *b* = 0.3183 nm, *c* = 0.4652 nm; Figure 2a). After 6.0 and 12 h, the solid products are mixtures of  $\beta$ -Co(OH)<sub>2</sub> and cubic spinel (Figure 2b,c), and after 18 and 24 h, a pure spinel phase is formed (Figures 2d and 1a). The results indicate that there is a gradual replacement of the kinetically formed brucite-like cobalt hydroxide by spinel oxide during autoclaving aging.

The zinc content in the solids varies with the reaction time (Figure S1 in the Supporting Information). No zinc content was detected by EDS for the product after 3.0 h of reaction because

- (18) (a) Song, Q.; Zhang, Z. *J. Am. Chem. Soc.* **2004**, *126*, 6164–6168. (b) Lin, C. K.; Li, Y. Y.; Yu, M.; Yang, P. P.; Lin, J. *Adv. Funct. Mater.* **2007**, *17*, 1459–1465. (c) Feldmann, C. *Adv. Funct. Mater.* **2003**, *13*, 101–107. (d) Sharma, Y.; Sharma, N.; Rao, G. V. S.; Chowdari, B. V. R. *Adv. Funct. Mater.* **2007**, *17*, 2855–2861. (e) Hou, Y. L.; Kondoh, H.; Shimojo, M.; Kogure, T.; Ohta, T. *J. Phys. Chem. B* **2005**, *109*, 19094–19098. (f) Chen, H. M.; Liu, R. S.; Li, H. L.; Zeng, H. C. *Angew. Chem., Int. Ed.* **2006**, *45*, 2713–2717. (g) Liu, X. H.; Qiu, G. Z.; Li, X. G. *Nanotechnology* **2005**, *16*, 3035–3040. (h) Niu, X. S.; Du, W. P.; Du, W. M. *Sens. Actuators, B* **2004**, *99*, 405–409. (i) Kim, H. J.; Song, I. C.; Sim, J. H.; Kim, H.; Kim, D.; Ihm, Y. E.; Choo, W. K. *J. Appl. Phys.* **2004**, *95*, 7387–7389.
- (19) Krezhov, K.; Konstantinov, P. *J. Phys.: Condens. Matter* **1993**, *5*, 9287–9294.
- (20) (a) Nethravathi, C.; Sen, S.; Ravishankar, N.; Rajamathi, M.; Pietzonka, C.; Harbrecht, B. *J. Phys. Chem. B* **2005**, *109*, 11468–11472. (b) Ilic, A.; Antic, A.; Poleti, D.; Rodic, D.; Prelevic, I. P.; Karanovic, L. *J. Phys.: Condens. Matter* **1996**, *8*, 2317–2325. (c) Ichianagi, Y.; Yamada, S. *Polyhedron* **2005**, *24*, 2813–2816.

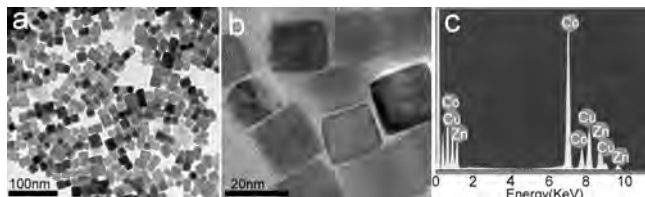


**Figure 3.** (a) Low-magnification and (b) high-magnification TEM micrographs showing the nanocubes synthesized at 180 °C for 18 h. (c) Related EDS spectrum from the particles.

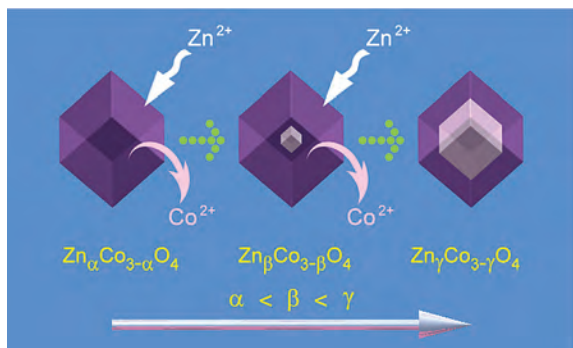


**Figure 4.** Schematic illustration of the nanoscale differential diffusion (cation exchange) and the hollowing process.

it is pure cobalt hydroxide. The absence of zinc in the solid product at this growth stage may be attributed to the stability of tetrahedral  $[\text{Zn}(\text{NH}_3)_4]^{2+}$  and to the different coordination of zinc in it as compared to that in the brucite structure (for details, see the caption to Figure S1 in the Supporting Information). After 6.0 h of reaction, the solid spinel nanocrystals have begun to grow in a highly oriented manner on the surface of the hexagonal  $\beta\text{-Co}(\text{OH})_2$  plates (for details, see Figures S2 and S3 in the Supporting Information). At this stage of growth, a negligible zinc content was also detected (Figure S2 in the Supporting Information), indicating that the initial solid nanoparticles grown on  $\beta\text{-Co}(\text{OH})_2$  are spinel with close to pure  $\text{Co}_3\text{O}_4$  composition.

Microscopic examination of the products from 12 h of reaction indicates that more spinel cubes were formed in accordance with the powder XRD result (Figure 2c) and the solid spinel particles were found to have an increased zinc content (Figures S1c and S4 in the Supporting Information). These results indicate that cobalt is gradually substituted by zinc within the spinel phase. After continued reaction to 18 h, a pure spinel phase was obtained as well-defined crystalline nanocubes (Figure 3) and the Zn/Co atomic ratio measured by EDS was ca. 1:4. A few cubes with tiny hollow interiors became visible by TEM observation (Figures 3b and S5 in the Supporting Information). Upon further aging to 24 h, as shown in Figure 1, hollow cubes with larger cavities were obtained and the Zn/Co atomic ratio was further increased to ca. 1:3.

Because the  $\text{Co}_3\text{O}_4$  nanocubes grown on the  $\beta\text{-Co}(\text{OH})_2$  surface at an early stage are solid and the nanocrystals after further reaction gradually become hollow with increased zinc composition, it can be concluded that there is a differential diffusion between zinc and cobalt cations during the reaction. The growth procedure is schematically illustrated in Figure 4. Because the zinc ion, whose ionic radius in a tetrahedral environment is practically equal to that of a divalent cobalt ion

$[(r_{\text{Zn}^{2+}})_{\text{tetra}} = 0.60 \text{ \AA} \text{ and } (r_{\text{Co}^{2+}})_{\text{tetra}} = 0.58 \text{ \AA}]$ , prefers to be coordinated by four oxygen atoms in tetrahedral geometry (18-electron configuration),<sup>19</sup> the “substitution” of  $\text{Zn}^{2+}$  ions for  $\text{Co}^{2+}$  ions in the spinel lattice is practicable. The differential “ion exchange” of a fast out-diffusion and a less efficient in-diffusion of ions introduces a net mass transport between the internal and external parts of the spinel  $\text{Zn}_x\text{Co}_{1-x}\text{Co}_2\text{O}_4$  nanocubes. With continuing hollowing in the central part, an inner cavity is created. Unlike other examples in which the Kirkendall effect has been observed,<sup>4,5</sup> the present hollowing phenomenon occurs without phase change and the cubic geometry is maintained throughout the process. With the substitution of zinc for cobalt, the physical properties of the nanocubes, such as magnetic properties, can be tailored to some degree because the extent of substitution  $x$  varies over time (Figure S6 in the Supporting Information).

The hypothetical limit of substitution  $x = 1$  to form a pure phase  $\text{ZnCo}_2\text{O}_4$  has not yet been achieved in this system. With further reaction beyond 24 h, a new phase gradually appears, which apparently belongs to a hydrotalcite-like compound. The hollow nanocubes are gradually destroyed, and zinc ions are released back to the solution (Figure S7 in the Supporting Information). In addition to the reaction time, the growth of the hollow nanocubes is sensitive to other conditions such as the selection of cosolvent, additives, and the presence of zinc. Without zinc acetate in the starting feedstock, no hollow nanocubes can be isolated, indicating a significant role of zinc in the growth of the hollow spinel nanostructures and supporting the hypothesis that a nanoscale Kirkendall effect is at work.

In conclusion, we have presented evidence for the formation of hollow spinel nanocubes with single-crystal nanowalls of a ternary compound, zinc cobalt oxide. The synthesized hollow nanocubes with edge lengths of ca. 18 nm and wall thicknesses of ca. 6 nm are among the smallest hollow nanocubes of any compounds reported so far. Their formation appears to be due to nanoscale Kirkendall diffusion, in which interior  $\text{Co}^{2+}$  and exterior  $\text{Zn}^{2+}$  are ion-exchanged. During the differential diffusion and hollowing, both the cube geometry and spinel phase type are preserved. Further development and understanding of such nanoscale chemical diffusion processes should allow their use in rational and systematic approaches to tailoring interior nanostructures, chemical compositions, and consequently physical properties of a variety of nanomaterials.

**Acknowledgment.** This work is supported financially by the National Natural Science Foundation (NSF) of China and the Government of Guangdong Province for NSF (Grants U0734002, 20571087, and 5003273) and industry program (Grants 2006B14701002 and 2007B090400001). M.W. is grateful to Dr. W. L. Zhou at the University of New Orleans for helpful discussions.

**Supporting Information Available:** Additional structural illustrations, SEM images, TEM images, EDS spectra, and magnetic properties. This material is available free of charge via the Internet at <http://pubs.acs.org>.

IC702457B